

PONTIFICIA UNIVERSIDAD JAVERIANA



Pontificia Universidad
JAVERIANA
Colombia

MASTER THESIS

Dynamical Model Bio-inspired of the Human Body in Upright Position

Author:
Eng. German D. Montañez P.

Supervisors:
Ph.D. Diego A. Patiño G.
D.I. Martha Zequera D.

December 2015

ARTÍCULO 23 DE LA RESOLUCIÓN N^o 13 DE JUNIO DE 1946

“La universidad no se hace responsable de los conceptos emitidos por sus alumnos en sus proyectos de grado. Sólo velará porque no se duplique nada contrario al dogma y la moral católica y porque los trabajos no contengan ataques o polémicas puramente personales. Antes bien, que se vea en ellos el anhelo de buscar la verdad y la justicia”.

Contents

Contents	ii
1 Introduction	1
2 Upright Position Biomechanics	2
2.1 Antropometry	2
2.2 Ankle and Hip Bio-mechanics	2
2.3 Double Inverted Pendulum Model	4
3 Control of Center of Mass	7
3.1 Linear Quadratic Regulator (LQR)	7
3.2 Weighting Matrices	8
3.3 Control Simulation	9
4 Model States Estimation	11
4.1 Balance Sensors Dynamics	11
4.2 Kalman Filter	13
4.3 Observer Simulation	14
5 Natural Sway Simulation	16
5.1 Input Characterization	16
5.2 Simulation Results	16
6 Experiment Protocol	21
6.1 Participants Conditions	21
6.2 Measures	21
6.3 Validation and Adjustment	23
7 Conclusions and Future Work	24
Bibliography	25

1 | Introduction

As a consequence of the Diabetes, the heart muscles loss capacity. This condition hinders the blood flux especially in parts of the body furthest from the heart causing weakness in the tissues of the feet. The modification of the tissues properties can produce a change in the normal pressure pattern in the feet, causing changes in the charge distribution in the areas of support that can influence to keep up the stability in upright posture [1].

The BASPI group of electronics engineering department has the "Footlab" laboratory, in Atico center. An analysis of diabetic patients is being implemented in this laboratory in order to develop orthopedic insoles to correct changes of the foot features and, in this way, redistribute the pressure point to prevent ulcers.

In order to design and test those insoles, it is necessary a complete analysis of the plantar pressure and the characteristics of the equilibrium of the patient. For this reason, the analysis of the postural balance control was proposed as a part of the studies of equilibrium because changes produced by the insoles could affect the equilibrium of the upright position.

The principal objective of this project is to model the upright position of the adult persons between 20 to 25 years old by approximating the human body to double joint pendulum. In order to achieve this objective the next specific objectives were selected as follows:

- To approximate the model of double joint pendulum to describe the upright position of the adult person between 20 to 25 years old.
- To do the basic engineering to select the necessary sensors to measure the posture based on the model.
- To determine the controllability of the posture based on the model, and if it is possible, determine a control law that ensure stability taking into account the stability and perturbations reject.
- To validate the results with simulations in order to contrast the mechanical model with simmechanics.

In this project, a first approximation of the study of stability based on a dynamical model of human body is proposed. In this approximation, the normality of equilibrium will be studied and the behavior of the normal upright position will be defined by modeling the characteristics of the healthiest population (people between 20 to 25 years old [2]).

After the introduction, chapter 2 summarizes the upright position biomechanics, the selection criteria of the double inverted pendulum as an approximate model and presents the model equations based in the human body characteristics. In chapter 3, the control law is implemented in order to stabilize the model based on the states estimation. Chapter 4 shows the characterization of the natural sensors in the human body for keeping the balance and describes how the states are estimated taking into account the dynamic performance of those sensors. Chapter 5 analyzes the results of the model and explains the interpretation. Chapter 6 explains the methods to validate the model and how to proceed with measurements. A final chapter concludes.

2 | Upright Position Biomechanics

The human movement analysis requires kinetic measures as well: masses, moments of inertia, and their locations. In order to identify the main measurements to approximate the human body to a double link inverted pendulum it was necessary an anthropocentric study.

On the other hand, choosing the approximated model is crucial in order to achieve a correct interpretation of the study. In this part, a summary about the upright position biomechanics is presented taking into account the analysis of the grades of freedom and the main features of the body in order to get a dynamical model to describe the behavior of the upright position. Another fact is the distinction between men and women, an study about the gender differences in the postural sway addressed in [3] concludes that there are no significant differences.

2.1 Antropometry

First of all, the model was defined with a study about fundamental characteristics involved in the description of upright position. In this case, the most important features are the length and weight of the human body.

The analysis of the length and weight was realized using anthropometric tables. Since a necessary condition to apply the anthropometry tables is the weight, the percentage of fat and the percentage of water are within the normal parameters [4].

The basic dimension is the length of the segments between each joint. The figure 2.1 shows the standard anthropometric measures as a fraction of the body height. Also, the figure 2.2 summarizes the different body sections expressed in terms of the weight.

For the upright position, the most significant parts of the body are divided in two sections: from ankle to hip and from hip to head, taking as principal joints the ankle and hip. Using the figures 2.1 and 2.2 it is possible to know the mass and length of each body part as a percentage of total mass(M) and total height(H). The values taken in this study for the model are: HAT (Head, Arms and Trunk) $0.678M - 0.47H$ and legs $(2 * 0.161)M - 0.491H$; those values represent the length and weight of the segment comprehended between the hip and head and the segment between the ankle and hip respectively. The mass of the feet do not interfere in the system dynamics because the ankle is the pivot joint since in the process to keep the balance only interfere the mass of the body over the ankle [6].

2.2 Ankle and Hip Bio-mechanics

In [7] a study of the contribution of the hip and ankle joints to the balance control was made. During the measures of the upright position, the authors realize that each of those joints contribute to keep the body in upright position. Also, the movement is more significant sagittal than frontal, and the ankle joint do more effort than the hip-joint.

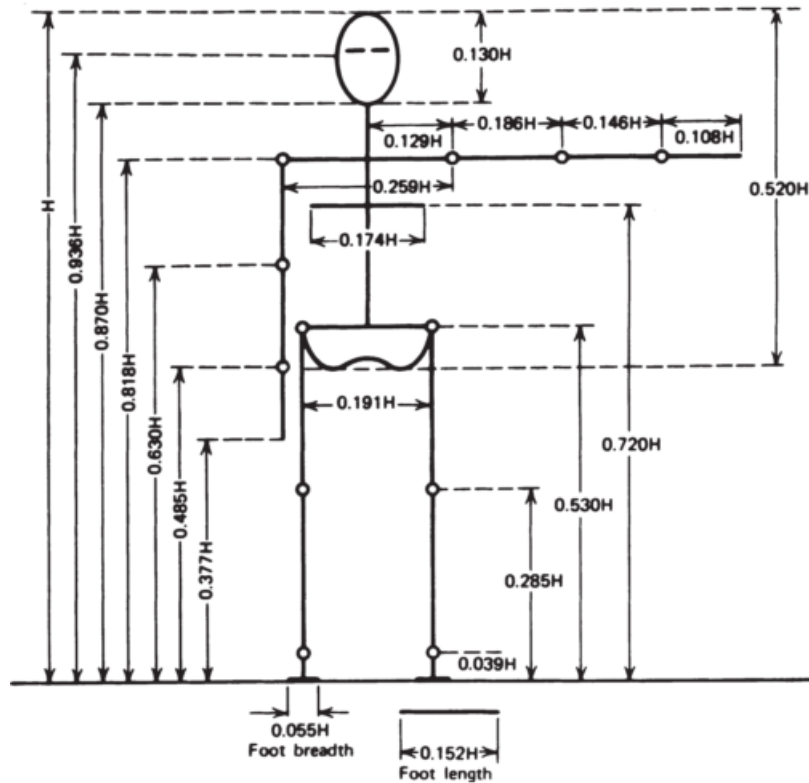


FIGURE 2.1: Body segment lengths expressed as a fraction of body height H [5].

Segment	Definition	Segment Weight/Total Body Weight	Center of Mass/Segment Length		Radius of Gyration/Segment Length			Density
			Proximal	Distal	C of G	Proximal	Distal	
Hand	Wrist axis/knuckle II middle finger	0.006 M	0.506	0.494 P	0.297	0.587	0.577 M	1.16
Forearm	Elbow axis/ulnar styloid	0.016 M	0.430	0.570 P	0.303	0.526	0.647 M	1.13
Upper arm	Glenohumeral axis/elbow axis	0.028 M	0.436	0.564 P	0.322	0.542	0.645 M	1.07
Forearm and hand	Elbow axis/ulnar styloid	0.022 M	0.682	0.318 P	0.468	0.827	0.565 P	1.14
Total arm	Glenohumeral joint/ulnar styloid	0.050 M	0.530	0.470 P	0.368	0.645	0.596 P	1.11
Foot	Lateral malleolus/head metatarsal II	0.0145 M	0.50	0.50 P	0.475	0.690	0.690 P	1.10
Leg	Femoral condyles/medial malleolus	0.0465 M	0.433	0.567 P	0.302	0.528	0.643 M	1.09
Thigh	Greater trochanter/femoral condyles	0.100 M	0.433	0.567 P	0.323	0.540	0.653 M	1.05
Foot and leg	Femoral condyles/medial malleolus	0.061 M	0.606	0.394 P	0.416	0.735	0.572 P	1.09
Total leg	Greater trochanter/medial malleolus	0.161 M	0.447	0.553 P	0.326	0.560	0.650 P	1.06
Head and neck	C7-T1 and 1st rib/ear canal	0.081 M	1.000	— PC	0.495	0.116	— PC	1.11
Shoulder mass	Sternoclavicular joint/glenohumeral axis	—	0.712	0.288	—	—	—	1.04
Thorax	C7-T1/T12-L1 and diaphragm*	0.216 PC	0.82	0.18	—	—	—	0.92
Abdomen	T12-L1/L4-L5*	0.139 LC	0.44	0.56	—	—	—	—
Pelvis	L4-L5/greater trochanter*	0.142 LC	0.105	0.895	—	—	—	—
Thorax and abdomen	C7-T1/L4-L5*	0.355 LC	0.63	0.37	—	—	—	—
Abdomen and pelvis	T12-L1/greater trochanter*	0.281 PC	0.27	0.73	—	—	—	1.01
Trunk	Greater trochanter/glenohumeral joint*	0.497 M	0.50	0.50	—	—	—	1.03
Trunk head neck	Greater trochanter/glenohumeral joint*	0.578 MC	0.66	0.34 P	0.503	0.830	0.607 M	—
Head, arms, and trunk (HAT)	Greater trochanter/glenohumeral joint*	0.678 MC	0.626	0.374 PC	0.496	0.798	0.621 PC	—
HAT	Greater trochanter/mid rib	0.678	1.142	—	0.903	1.456	—	—

*NOTE: These segments are presented relative to the length between the greater trochanter and the glenohumeral joint.
 Source Codes: M, Dempster via Miller and Nelson; *Biomechanics of Sport*, Lea and Febiger, Philadelphia, 1973. P, Dempster via Plagenhoef; *Patterns of Human Motion*, Prentice-Hall, Inc. Englewood Cliffs, NJ, 1971. L, Dempster via Plagenhoef from living subjects; *Patterns of Human Motion*, Prentice-Hall, Inc., Englewood Cliffs, NJ, 1971. C, Calculated.

FIGURE 2.2: Body segment expressed as a fraction of body height H and mass M [5].

While a human being is in up right position, the ankle and hip have restricted movements. And, as a natural response, the human body performs a dynamical equilibrium called sway. The characterization of this sway movements evidences that this movement is restricted to $\pm 6^\circ$ for the ankle and $\pm 5^\circ$ for the hip, and the maximum torque are $\pm 20Nm$ for the ankle and $\pm 15Nm$ for the hip ¹[8][7][9].

2.3 Double Inverted Pendulum Model

The inverted pendulum has been the basis of the analysis of the postural behavior as a dynamical model. Using the model of double joint pendulum it was possible to design a controller in order to keep the upright position of a paraplegic person. Also, through the measures of muscle effort in the ankle, the person can change the balance reference for the control [8].

Due to the human body complexity, many approximation have been developed, in some cases the model has been approximated as a single inverted pendulum, but not only the ankle contribute in the balance control. The double link pendulum adds the contribution of hip in the model dynamics [6][7][10]. Although the knee contribute to the natural sway, its contribution is not significant in standing, in [11] is demonstrated that the most significant contribution of the knees is presented in external perturbations and, in this project, external perturbations are not considered.

The human body, in upright position, it is more stable in frontal orientation than the sagittal orientation. In frontal orientation, the human body has two points of support (both feet), and the distance between the feet allows more control, but in sagittal orientation the body only has one support point and the control depends totally of the ankle muscles. For this reason the model of inverted pendulum was analyzed only in sagittal orientation[12].

In this project, the approximation of double link pendulum was selected as a model of the human being. Based on the figure 2.3, we develop the model equations.

The kinetic and potential energy of system is:

$$K = \frac{1}{2}(m_1((l_1\dot{\theta}_1 \cos(\theta_1))^2 + (l_1\dot{\theta}_1 \sin(\theta_1))^2) + m_2((l_1\dot{\theta}_1 \cos(\theta_1) + l_2\dot{\theta}_2 \cos(\theta_2))^2 + (l_1\dot{\theta}_1 \sin(\theta_1) + l_2\dot{\theta}_2 \sin(\theta_2))^2)) \quad (2.1)$$

$$P = g(m_1l_1 \cos(\theta_1) + m_2(l_1 \cos(\theta_1) + l_2 \cos(\theta_2)))$$

where, θ_1 is the ankle angle respect to the vertical axis, θ_2 is the hip angle respect to the vertical axis, l_1 is the distance between the ankle and the hip, l_2 is the distance between the head and the hip, m_1 is the mass of the segment between the hip and the ankle, m_2 is the mass of the segment between the head and the hip, and g is the gravity constant. Based on the anthropometric studies, for each segment the values of the lengths and weights are expressed in terms of the total weight (M) and the total length (H) of the body: $l_1 = 0.491H$, $l_2 = 0.47H$, $m_1 = (2 * 0.161)M$ and $m_2 = 0.678M$.

¹This restrictions are conditioned to sagittal view. Also, are the maximum value for the sway.

$$L = K - P$$

$$\frac{d}{dt} \frac{\partial L}{\partial \dot{\theta}_i} - \frac{\partial L}{\partial \theta_i} = 0 \quad (2.2)$$

Using the analysis of the potential (P) and kinetic (K) energy, and replace it on the Lagrange equation (2.2) the result of the system is:

$$\begin{aligned} \ddot{\theta}_1 &= \frac{-(l_1 m_2 \cos(\theta_1 - \theta_2) \sin(\theta_1 - \theta_2) \dot{\theta}_1^2 + l_2 m_2 \sin(\theta_1 - \theta_2) \dot{\theta}_2^2 - g m_1 \sin(\theta_1) - g m_2 \sin(\theta_1) + g m_2 \cos(\theta_1 - \theta_2) \sin(\theta_2))}{(l_1(m_1 + m_2 - m_2 \cos(\theta_1 - \theta_2))^2)} \\ \ddot{\theta}_2 &= \frac{g m_1 \sin(\theta_2) + g m_2 \sin(\theta_2) + \dot{\theta}_1^2 l_1 m_1 \sin(\theta_1 - \theta_2) + \dot{\theta}_2^2 l_1 m_2 \sin(\theta_1 - \theta_2) - g m_1 \cos(\theta_1 - \theta_2) \sin(\theta_1)}{(l_2(m_1 + m_2 - m_2 \cos(\theta_1 - \theta_2))^2)} \\ &\quad + \frac{-g m_2 \cos(\theta_1 - \theta_2) \sin(\theta_1) + \dot{\theta}_2^2 l_2 m_2 \cos(\theta_1 - \theta_2) \sin(\theta_1 - \theta_2)}{(l_2(m_1 + m_2 - m_2 \cos(\theta_1 - \theta_2))^2)} \end{aligned} \quad (2.3)$$

In equilibrium state, the angles and the inputs of the system are zero. The equations (2.3) were linearized in *Matlab*² and resulting matrices are:

$$\begin{aligned} \dot{X} &= AX + BU \\ Y &= CX + DU \end{aligned} \quad X = \begin{bmatrix} \theta_1 \\ \dot{\theta}_1 \\ \theta_2 \\ \dot{\theta}_2 \end{bmatrix} \quad U = \begin{bmatrix} T_1 \\ T_2 \end{bmatrix} \quad (2.4)$$

$$\begin{aligned} A &= \begin{bmatrix} 0 & 1 & 0 & 0 \\ \frac{gm_1 + gm_2}{l_1 m_1} & 0 & -\frac{gm_2}{l_1 m_1} & 0 \\ 0 & 0 & 0 & 1 \\ -\frac{gm_1 + gm_2}{l_2 m_1} & 0 & \frac{gm_1 + gm_2}{l_2 m_1} & 0 \end{bmatrix} \\ B &= \begin{bmatrix} 0 & 0 \\ \frac{1}{l_1 m_1} & -\frac{1}{l_2 m_1^2} \\ 0 & 0 \\ -\frac{1}{l_1 m_1 m_2} & \frac{1}{l_2 m_1} \end{bmatrix} \quad C = \begin{bmatrix} 1 & 0 & 0 & 0 \\ 0 & 0 & 1 & 0 \end{bmatrix} \end{aligned} \quad (2.5)$$

²The complete procedure is showed in the Annexes/Simulation/control pen.m in the section of the code labeled: Linearization

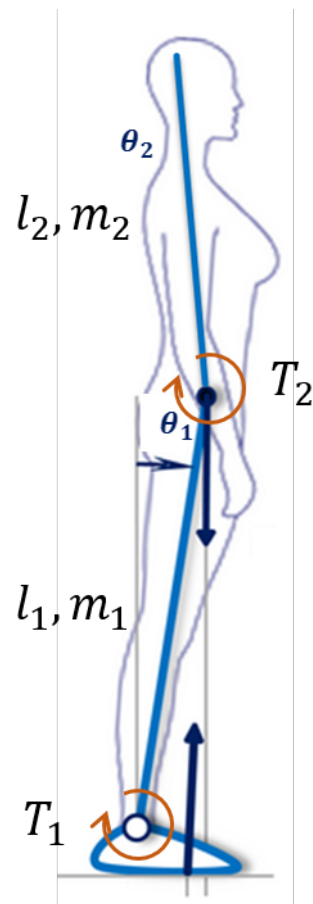


FIGURE 2.3: Human double pendulum approximation.

3 | Control of Center of Mass

To analyze the balance control is used the center of mass, the center of pressure or both but, for different positions of the body is possible to get same measure of those variables. In the figure 3.1 shows that for different position, the center of mass and the center of pressure are the same, for example in the positions 1 and 4 in the figure the center of mass is the same but the position and the displacement direction are different, also in the positions 2 and 3 the center of pressure is the same but the the position and the displacement direction are different[5]. In this project is proposed another approximation for evaluate the human balance taking the state variables in order to get more information about the behavior of the body in upright position.

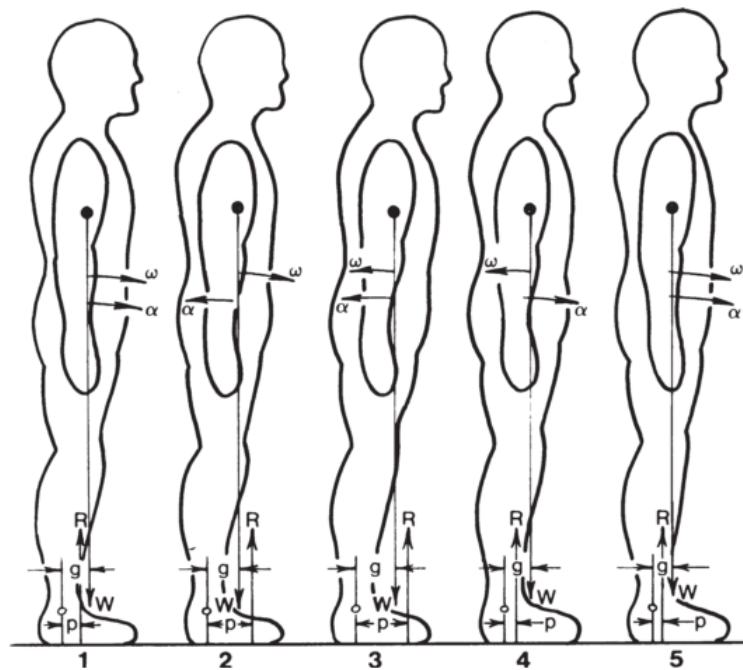


FIGURE 3.1: Different position of the poses in natural sway. R represent the center of mass and W the center of pressure[5].

Experimental evidence suggests that states information is used in selection of control strategy. Due that the control objective is to keep the equilibrium point, a Linear Quadratic regulator (LQR) was implemented. In addition, this technique provides the optimal gains for control, it is similar to the human body process due to the fact that the control balance is based in the information about the position of the human body parts and the process is optimized during growth[13][14].

3.1 Linear Quadratic Regulator (LQR)

This is the most fundamental form of control for linear systems because it uses the principal action of control: each state is multiplied by a gain to feedback the system.

In order to find the vector of gains (K) a Linear Quadratic Regulator (LQR) was implemented. This method consists on making the transition from the initial state $x(k_0)$ to the final state $x(k) = 0$ using the control function $u(k) = Kx(k)$ [15].

$$\min_{u(t)} \int_0^{\infty} (x(t)^T Q x(t) + u(t)^T R u(t)) dt \quad (3.1)$$

In this case, the control objective is to keep the equilibrium in the double inverted pendulum with the less quantity of energy. Also, the weighing matrices R and Q of (3.1) can be chosen to penalize excessive exertion of control effort and undesired excursions of the state from stable upright position[13].

Based on [16], the values of the matrices Q and R were chosen.

3.2 Weighting Matrices

The matrix R affects directly the penalization of the ankle and hip exertion, in this case, the relative cost of both signals is the same. For those reasons the value of R is:

$$R = I_{2 \times 2} \quad (3.2)$$

The matrix Q penalizes variations in the states, in order to get a convergent result the matrix must be defined positive. The criteria to find the value of Q is shown below.

$$Q' = \sigma^2 \frac{\mu Q_{cm} + (1 - \mu) Q_{up}}{\lambda_{max}(\mu Q_{cm} + (1 - \mu) Q_{up})} \quad (3.3)$$

In the equation (3.3), σ value represent the effort of the control, λ_{max} is the maximum singular value of the matrix A , Q_{cm} represents the penalization caused by move restrictions in the hip and ankle angles as changes in center of mass, Q_{up} penalize the variation in the hip and ankle angles in order to keep standing, and μ is value that interfere in the relationship between Q_{up} and Q_{cm} to add importance to keep the position or keep the restrictions. The values were characterised experimentally in [13] and each parameter are showed in table 3.1 and the values of Q_{up} and Q_{cm} are shown in the equation (3.4).

TABLE 3.1: Body mass as a fraction of body weight(M).[5]

Parameter	Value
σ	1
μ	0.5
λ_{max}	7.9798

$$\begin{aligned}
 Q_{cm} &= \begin{bmatrix} 0.57 & 0.17 \\ 0.17 & 0.05 \end{bmatrix} & Q_{up} &= \begin{bmatrix} 1.45 & -1.18 \\ -1.18 & 0.96 \end{bmatrix} \\
 Q &= \begin{bmatrix} Q' & 0 \\ 0 & 0 \end{bmatrix}
 \end{aligned} \tag{3.4}$$

The optimization problem was solved with *Matlab* in order to find the value of K .

3.3 Control Simulation

In this case we control the center of mass indirectly through the ankle and hip forces.

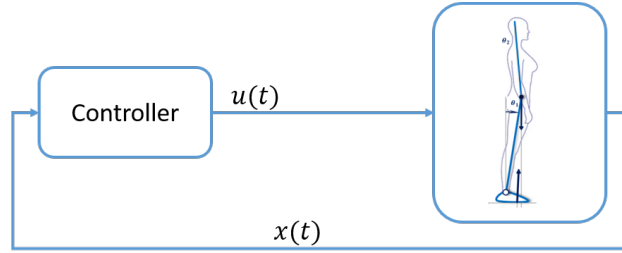


FIGURE 3.2: Block Diagram of the balance control approximation.

Finally the figure 3.2 shows the block diagram of the balance control approximation using as controller the LQR designed. The signal $u(t)$ corresponds to the control signals, the force of the hip and ankle, $x(t)$ are the states of the double inverted pendulum model.

The controller was tested with the linear model and the non linear model in *Simulink*. The figure 3.3 and 3.4 show the control performance, the blue line is the lineal model and the green line is the non linear model. This test was performed with the following parameters: $M = 75kg$, $H = 1.75m$; and the initial conditions: $\theta_1 = 1^\circ$ $\theta_2 = -1^\circ$ $\dot{\theta}_1 = 0^\circ$ $\dot{\theta}_2 = 0^\circ$. There is an error between the signals because the nonlinearity but the control can stabilize both models.

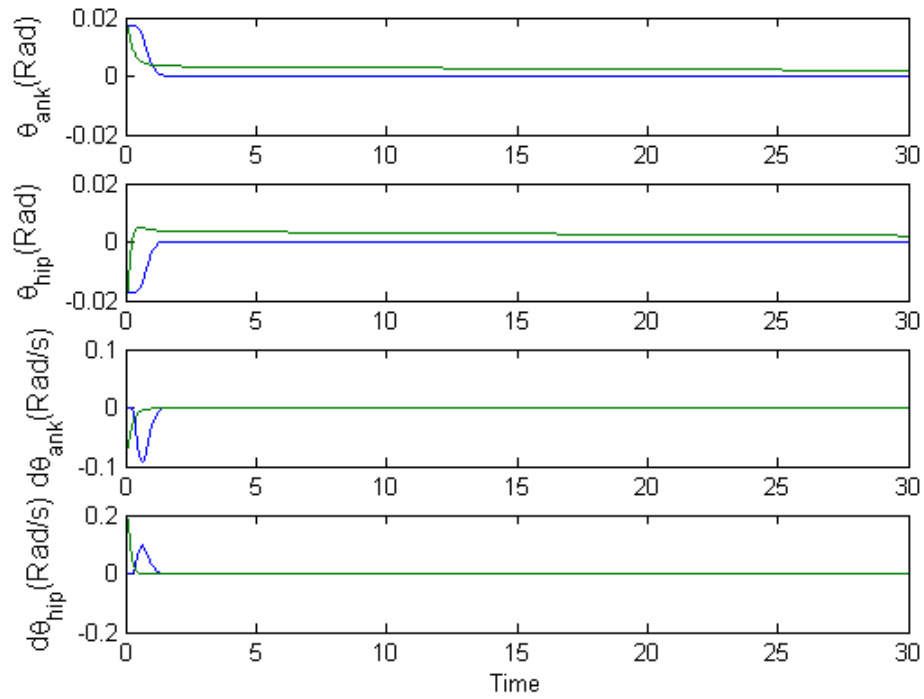


FIGURE 3.3: System response with the LQR controller. The blue line is the lineal model, the green line is the non linear model.

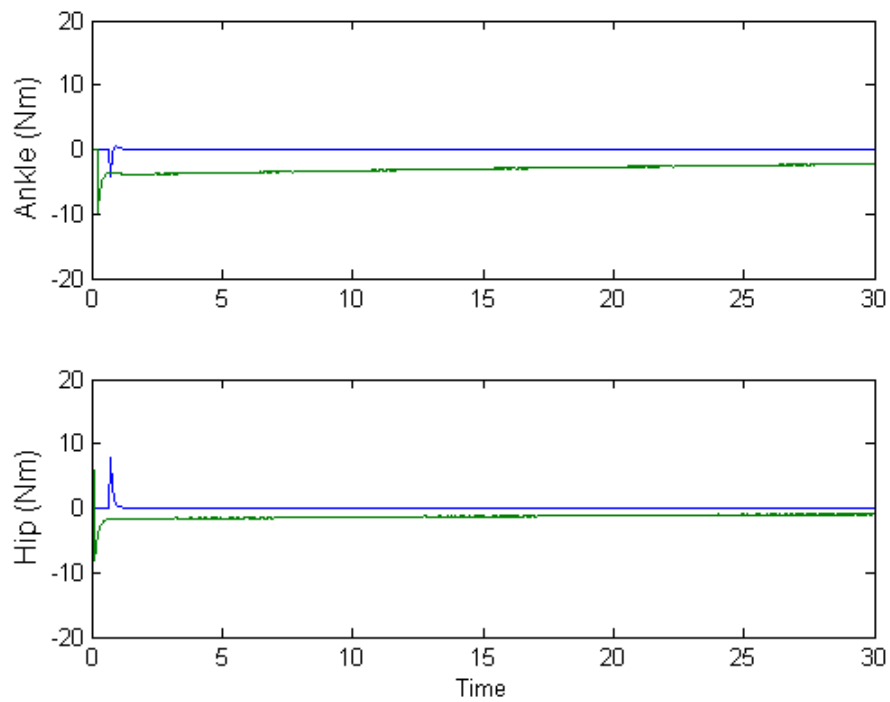


FIGURE 3.4: Control signal with the LQR controller. The blue line is the lineal model, the green line is the non linear model.

4 | Model States Estimation

By modeling the natural sensors of the body in charge to measure the deviations of balance, it is possible to develop a simulation of the effects of deterioration in the sensors. This allows us to predict how this effect could interfere in the equilibrium of people in the case of some sensors fail. We decided to add the behavior of the natural sensors of the body in order to estimate the space state variables.

4.1 Balance Sensors Dynamics

In balance control, other variables contribute to keep the upright position. The double inverted pendulum takes into account the basic physic behavior of the human body, but the dynamics of the sensors that allows us to keep balance must be added to the model.

The principal sensors are related to: the proprioception, visual rotation and translation, and vestibular rotation and translation. Each sensor was analysed as a dynamical system in state space form.

$$\begin{aligned} \dot{x}_s &= A_s x_s + B_s u_s \\ y_s &= C_s x_s + D_s u_s \end{aligned} \quad (4.1)$$

In the equation (4.1), y_s represent the output of the sensor, u_s the stimulus of the sensors, and x_s represents the states of the sensors. Then, the dynamical model of the sensors is attached to the double inverted pendulum model.

In accordance to [5], the proprioception signals sent by the muscles in the joint, in this case are two signals, one for the ankles and other for the hip. Regarding to the vestibular sensors, the human body has two groups of organs to sense the acceleration, one is the semicircular canal inside the ear and the otoliths. Finally, for the visual rotation and translation the model is limited by two degrees of freedom. The final states are:

$$X_{BS}^T = [x_B^T \ x_{ap}^T \ x_{hp}^T \ x_{sc}^T \ x_{ot}^T \ x_{vr}^T \ x_{vt}^T] \quad (4.2)$$

where, x_B represent the states of the linearized double inverted pendulum model, x_{ap} and x_{hp} represents the states for the propiacement sensors of the ankles and the hip, x_{sc} and x_{ot} are the states for the vestibular sensors divided in semicircular canals and the otholits respectively, and x_{vr} and x_{vt} are the states for the visual rotation and the visual translation.

For the propiacement sensors , the signal is generated by the muscles in the ankles and the hip and it can be modeled as a lead lag control which provide a signal proportional to length and velocity within a limited bandwidth[17].

$$\begin{aligned} A_{ap} = A_{hp} &= \frac{-1}{\alpha T_{sp}} & B_{ap} = B_{hp} &= \frac{1}{\alpha T_{sp}} \\ C_{ap} = C_{hp} &= \frac{\alpha - 1}{\alpha} & D_{ap} = D_{hp} &= \frac{1}{\alpha} \end{aligned} \quad (4.3)$$

The equation (4.3) shows the matrices for each proprioception sensor. The inputs of the sensors are the ankle and hip joint angles $u_{ap} = \theta_1$, $u_{hp} = \theta_2 - \theta_1$. The constants T_{sp} and α represent the parameters in the lead-lag transfer function. In [17] a study about the muscle spindles find that the values of the parameters $T_{sp} = 0,4$ and $\alpha = 0.15$.

The semicircular canal has an overdamped response to the angular acceleration which is detected by hair cells whose firing rate is roughly proportional to angular velocity [18]. Based on [16] the equation (4.4) describes the behavior of semicircular canal sensors.

$$\frac{Y_{sc}}{X_{angacc}} = \frac{k_{sc}s(s + \omega_{s1})}{(s + \omega_{s2})(s + \omega_{s3})} \quad (4.4)$$

The values of the parameters in the equation are: $k_{sc} = 0.574$, $\omega_{s1} = 100$, $\omega_{s2} = 0.1$ and $\omega_{s3} = 0.033$.

The otoliths performance are described by the equation (4.5).

$$\frac{Y_{ot}}{X_{linacc}} = \frac{k_{ot}(s + \omega_{o1})}{s + \omega_{o2}} \quad (4.5)$$

where, $k_{ot} = 90$, $\omega_{o1} = 0.1$ and $\omega_{o2} = 0.2$ [19].

And for the visual rotation and translation a simplified model for visual signal processing was implemented with a bandwidth limitation.

$$\frac{Y_v}{X_v} = \frac{1}{T_v s + 1} \quad (4.6)$$

The equation (4.6) represents the performance of the visual sensors and the value of the parameter $T_{vs} = 0.1$ [16].

Once all the sensors are written in in state space form, the model extended with the sensors dynamics is:

$$\begin{aligned}
 A_{BS} &= \begin{bmatrix} 0 & I_{2 \times 2} & & & & & & & \\ G & 0 & & & & & & & \\ B_{ap}f_1^T & & A_{ap} & & & & & & \\ B_{hp}f_2^T & & & A_{hp} & & & & & \\ B_{sc}g_2^T & & & & A_{sc} & & & & \\ B_{ot}c_t^T g_1^T & & & & & A_{ot} & & & \\ & B_{vr}f_2^T & & & & & A_{vr} & & \\ & B_{vt}c_t^T & & & & & & A_{vt} & \end{bmatrix} \\
 B_{BS} &= \begin{bmatrix} 0 \\ H \\ 0 \\ 0 \\ B_{sc}h_2^T \\ B_{ot}c_t^T h_1^T \\ 0 \\ 0 \end{bmatrix} \\
 C_{BS} &= \begin{bmatrix} I_{4 \times 4} & & & & & & & & \\ 0 & 0 & C_{ap} & & & & & & \\ 0 & 0 & & C_{hp} & & & & & \\ D_{sc}g_2^T & & & & C_{sc} & & & & \\ D_{ot}c_t^T g_1^T & & & & & C_{ot} & & & \\ 0 & 0 & & & & & C_{vr} & & \\ 0 & 0 & & & & & & C_{vt} & \end{bmatrix} \\
 D_{BS} &= \begin{bmatrix} 0 \\ 0 \\ D_{sc}h_2^T \\ D_{ot}c_t^T h_1^T \\ 0 \\ 0 \end{bmatrix}
 \end{aligned} \tag{4.7}$$

where,

$$\begin{aligned}
 G = \begin{bmatrix} g_1^T \\ g_2^T \end{bmatrix} &= \begin{bmatrix} \frac{gm_1+gm_2}{l_1m_1} & -\frac{gm_2}{l_1m_1} \\ -\frac{gm_1+gm_2}{l_2m_1} & \frac{gm_1+gm_2}{l_2m_1} \end{bmatrix} \quad H = \begin{bmatrix} h_1^T \\ h_2^T \end{bmatrix} = \begin{bmatrix} \frac{1}{l_1m_1} & -\frac{1}{l_2m_1^2} \\ -\frac{1}{l_1m_1m_2} & \frac{1}{l_2m_1} \end{bmatrix} \\
 F = \begin{bmatrix} f_1^T \\ f_2^T \end{bmatrix} &= \begin{bmatrix} 1 & 0 \\ -1 & 1 \end{bmatrix} \quad c_t = [c_{t1} \quad c_{t2}] = [-0.835 \quad -0.735]
 \end{aligned} \tag{4.8}$$

The equations (4.7) and (4.8) represent the model of the inverted pendulum with the dynamics of the human body sensors attached.

4.2 Kalman Filter

The estimate is produced by an internal model of the body and sensory dynamics. This model can produce both a state estimate \hat{x}_{BS} and a prediction \hat{y}_s of sensory output. Process noise and other disturbances can cause the actual state to deviate from this estimate. This deviation can

be corrected with feedback of the sensory prediction error $y_s - \hat{y}_s$, with estimator gain matrix L determining the effect of the corrections on each state: x_{BS} . The most important requirement being the stabilization of the estimation error $x_{BS} - \hat{x}_{BS}$. A kalman filter was developed as an estimator of the model states taking into account the variance of the natural sway.

The estimator not only computes the states variables, the sensor signals are estimated also. This allows to see the behavior of the signals which are used in the body to keep an upright position.

We assume that the measurement noise and the proses noise are not correlated. In [20] a study about the body sway characteristics shows that the noise in the measures can be modeled as Gaussian white noise and the matrices W and V for the proses noise and measurement noise respectively were:

$$W = \begin{bmatrix} 0.08 & 0 \\ 0 & 0.08 \end{bmatrix} \quad V = \begin{bmatrix} 1e^{-7} & 0 \\ 0 & 1e^{-7} \end{bmatrix} \quad (4.9)$$

Solving with Matlab the vector of gains for the optimal observer is:

$$L = \begin{bmatrix} 5525.81 & -214.62 \\ -214.62 & 10029.36 \\ 15290349.94 & -1669285.21 \\ -1669280.58 & 50317160.33 \\ 16.66 & -2.50e^{-5} \\ -16.66 & 16.66 \\ -1669252.04 & 50315826.42 \\ -214.67 & 10029.15 \\ -12760848.02 & 1185436.98 \\ -5730.44 & 10233.99 \\ -4447.95 & -7185.02 \end{bmatrix} \quad (4.10)$$

Using the estimated sensors signals is possible to generate the space state signals as linear combination of the output adding the contribution of each sensor to the space state estimation.

$$X_{LQR} = C_\theta X_{BS} = \begin{bmatrix} 1 & 0 & 0 & 0 & 1 & -1 & 0 & 0 & 0 & 0 \\ 0 & 1 & 0 & 0 & 0 & -1 & 0 & 0 & 0 & 0 \\ 0 & 0 & 1 & 0 & 0 & 0 & -0.01 & 0 & 0 & -1 \\ 0 & 0 & 0 & 1 & 0 & 0 & 0 & 0 & 1 & -1 \end{bmatrix} X_{BS} \quad (4.11)$$

The equation 4.11 shows the relation between the estimated states and the states of the double inverted pendulum model where, X_{LQR} represents the estimated states $[\hat{\theta}_1 \ \hat{\theta}_2 \ \hat{\theta}_1 \ \hat{\theta}_2]$.

4.3 Observer Simulation

Using the controller designed in the chapter 3, the performace of the observer was evaluated.

The figure 4.1 shows the block diagram of the observer intervention in the control performance. The signal $u(t)$ corresponds to the control signals (the force of the hip and ankle), $\hat{x}(t)$ are the

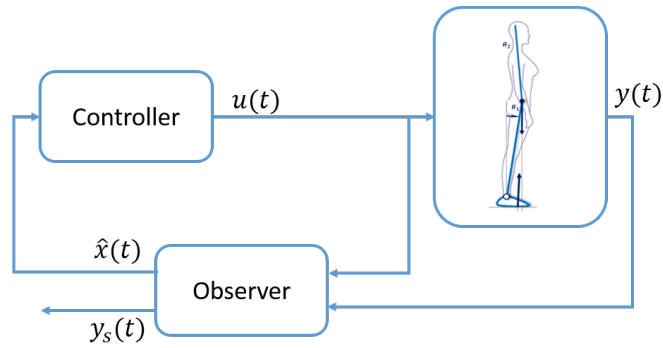


FIGURE 4.1: Block Diagram of the control-observer interaction.

estimated states of the double inverted pendulum model based on the measures of the hip and ankle joint $y(t)$ and $y_s(t)$ represents the estimated output of the signals provided by the natural sensors.

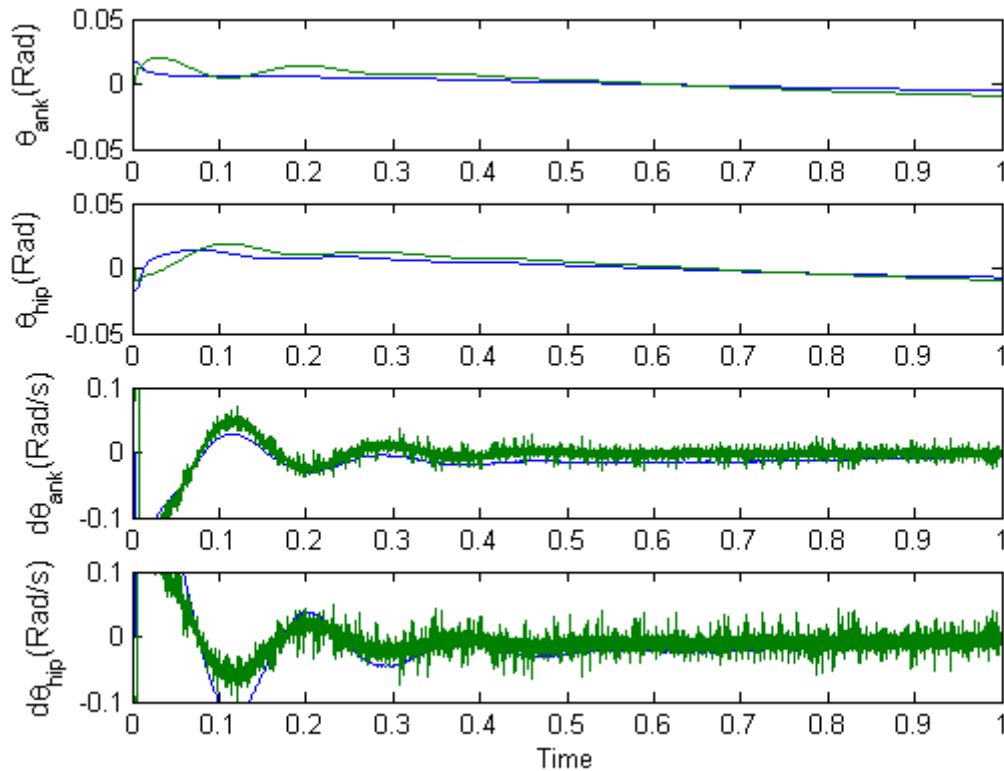


FIGURE 4.2: Control-Observer performance. The blue line is the state, the green line is the estimated state.

The figure 4.2 shows the control and the observer performance, the blue line is the state and the green line is the estimated state. This test was performed with the following parameters: $M = 75kg, H = 1.75m$; and the initial conditions: $\theta_1 = 1^\circ, \theta_2 = -1^\circ, \dot{\theta}_1 = 0^\circ, \dot{\theta}_2 = 0^\circ$ and zero for each state in the observer. The observer can reach the state signal in less than one second and also, the combination of the control and the observer can achieve the control objective.

5 | Natural Sway Simulation

In order to evaluate the model, a simulation about the natural sway is performed. The literature suggests that the natural sway increases with the age or some illnesses like parkinson or diabetes [7] [20]. For this reason the natural sway is used as a way to quantify the equilibrium [20][21][22].

The criteria used to introduce the data for simulations were selected taking into account the characteristics of an average person, that includes people in a age range 20-25 with necessary conditions to apply the anthropometric tables mentioned in the section 2.1.

5.1 Input Characterization

The control performance was probed adding Gaussian noise to the sensors signals estimated by the observer. The matrix of variances for each sensor is obtained by solving the equations in (5.1).

$$\begin{aligned} (A_{BS} - B_{BS}K_{BS})X_{cv} + X_{cv}(A_{BS} - B_{BS}K_{BS})^T + B_{BS}WB_{BS}^T &= 0 \\ Y = C_{BS}X_{cv}C_{BS}^T \quad V_o = [\pi_{ap} \quad \pi_{hp} \quad \pi_{sc} \quad \pi_{ot} \quad \pi_{vr} \quad \pi_{vt}]I_{6 \times 6} &Y \end{aligned} \quad (5.1)$$

where, X_{cv} is the state covariance, Y is the output covariance. The values for the sensor noise are $\pi_{ap} = 0.05$ $\pi_{hp} = 0.01$ $\pi_{sc} = 0.001$ $\pi_{ot} = 0.001$ $\pi_{vr} = 0.001$ $\pi_{vt} = 0.001$. Those values were taken from [16].

5.2 Simulation Results

For the simulation, the system only has the noise of the sensors as input signal and the test is applied with the parameters of a normal person also, the seed used to generate the noise signal is fixed in order to compare the results.

The figure 5.1 shows the model designed in *simmecanics*¹ to simulate the model behavior. In order to contrast the behavior of the model, the Roomberg test² was applied in the simulation. Due that the Roomber test requires evaluating the person with closed eyes, this sensors signals (x_{vr} , x_{vt}) were removed from the estimation.

For each simulation we analyzed the phase diagram between the angles θ_{Ankle} and θ_{Hip} . In order to summarize the dispersion of the data in this diagram the covariance ellipse is drawn with a 99%of confidence.

Taking as a reference a person with $M = 75kg$ and $H = 1.75mts$ the following results are presented.

The figure 5.2 shows the simulation results. The nonlinear model presents more sway than the linear model, in other words, the linear model is more stable than the non linear model.

¹*Simmecanics* is able to simulate the physical non linear behavior of the double inverted pendulum.

²upright standing for a minute, first with the eyes open, then with the eyes closed.

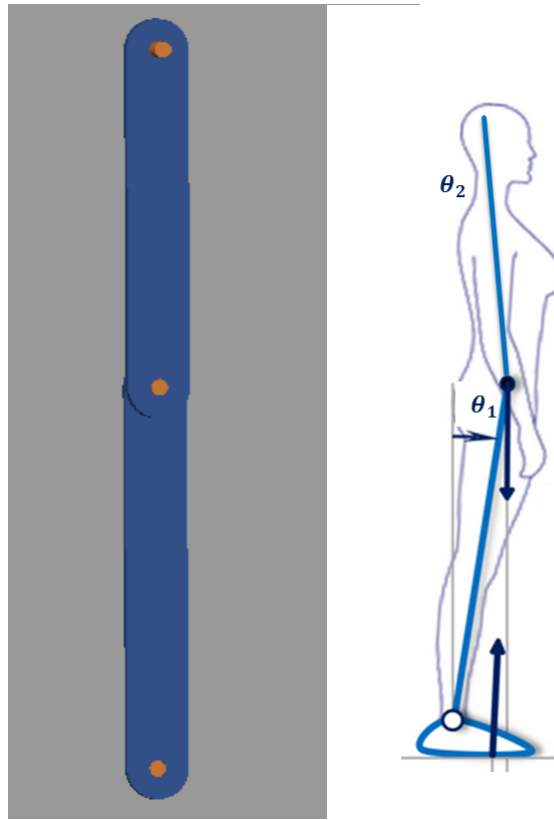


FIGURE 5.1: Simmechanics model.

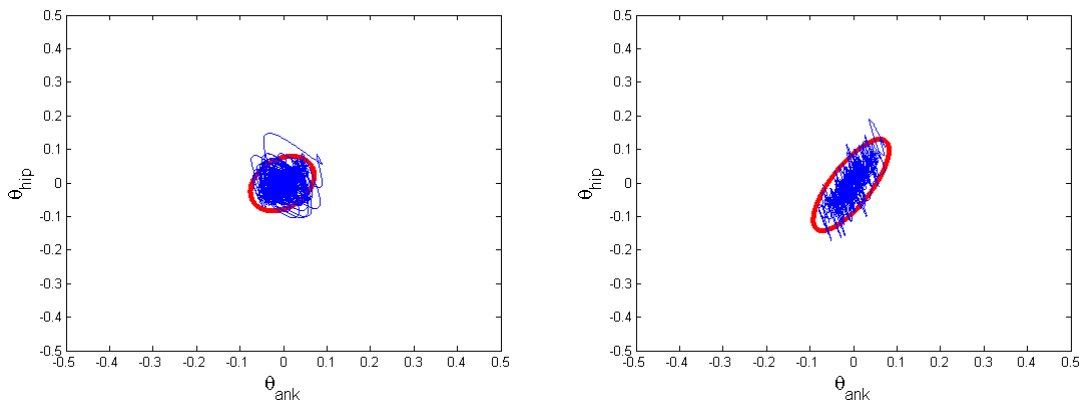


FIGURE 5.2: Linear (left) and nonlinear (right) simulation response. θ_{hip} and θ_{ank} are in degrees.

The figures 5.3 show the simulation of the Roomber's test with eyes open and closed respectively. The literature suggests that the dispersion of the measure of the natural sway with closed eyes is bigger than the measure with eyes opened. The figure 5.4 shows the comparison between the open eyes and closed eyes simulation. This figure is in accordance with the expected results regarding to [23][24] due to the fact that the increase in the angle is similar to the data shown in the right diagram in the figure. Also, the center of mass (COM) can be evaluated with the equation $x_{COM}(t) = 2.8\theta_1(t) + 2.8\theta_2(t)$ [24] and the figure 5.5 shows that the frequency response of the center of mass in the model has a similar behavior of the measures taken in [23].

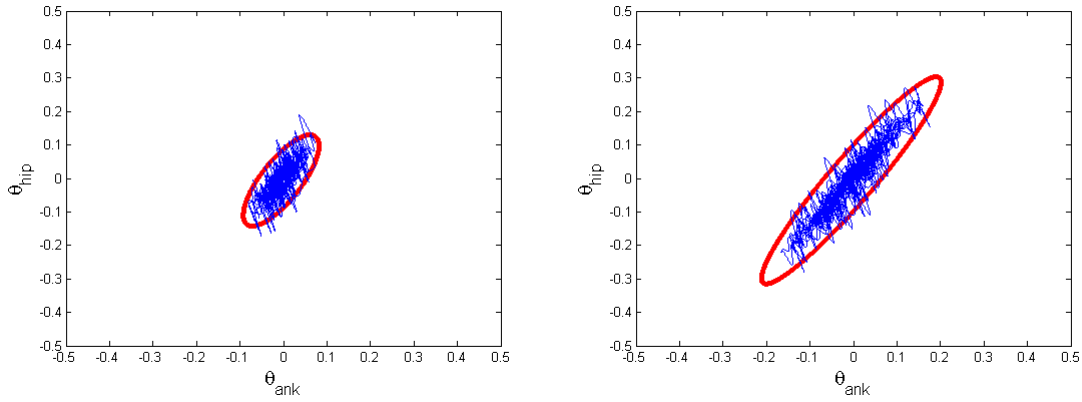


FIGURE 5.3: Simulated romberg test eyes open (left) closed eyes (right). θ_{hip} and θ_{ank} are in degrees.

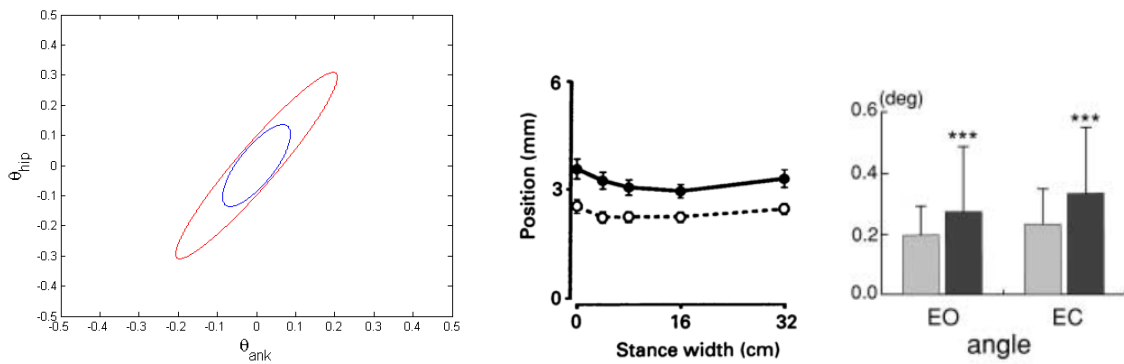


FIGURE 5.4: Comparison between the simulation whit eyes open in blue line and eyes closed in red line (left). θ_{hip} and θ_{ank} are in degrees. Figure taken from [23] shows the changes in the postural sway in sagittal position, the black circle represents the eyes closed, and the white circle the eyes open, the measure was taken with a marker in the shoulder in average people (middle). Figure taken from [24] shows the changes in the maximum amplitude in the ankle and hip sway with the eye open (EO) and the eyes closed (EC), in dark grey the hip and in light grey the ankle, the measure was taken in average people with laser sensors (right).

The figure 5.6 shows the effort in the control signal. The force applied in the ankle and hip do not exceed the range of normal operation (maximum torque are $\pm 20Nm$ [8][7][9]). Also, the control signal related with the closed eyes test (blue line) has more noise than the open eyes test (green line).

The figure 5.7 shows the states during the test. The signal have more variation during the the test with eyes closed (green line) than the test with the eyes open. The simulation of the natural sway with the open eyes and closed eyes is possible due that the estimation error increase without all input signals in the observer.

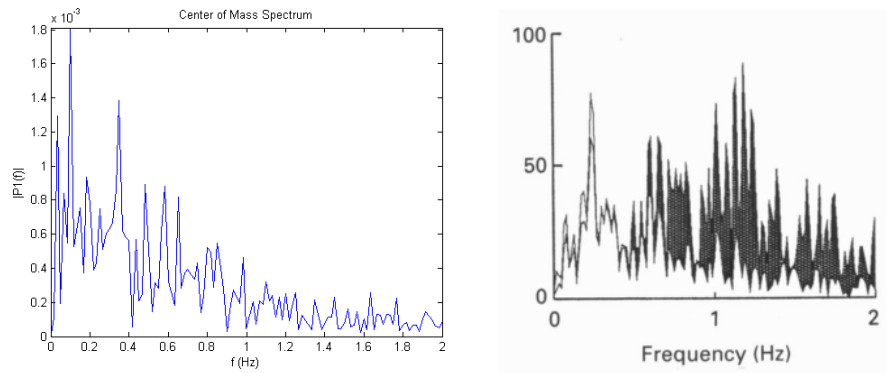


FIGURE 5.5: Frequency response of the center of mass for the open eyes test (left). Figure taken from [23] shows the frequency response of the center of mass in sagittal plane with open eyes, the shade represent the spectre of center of mass for frontal position

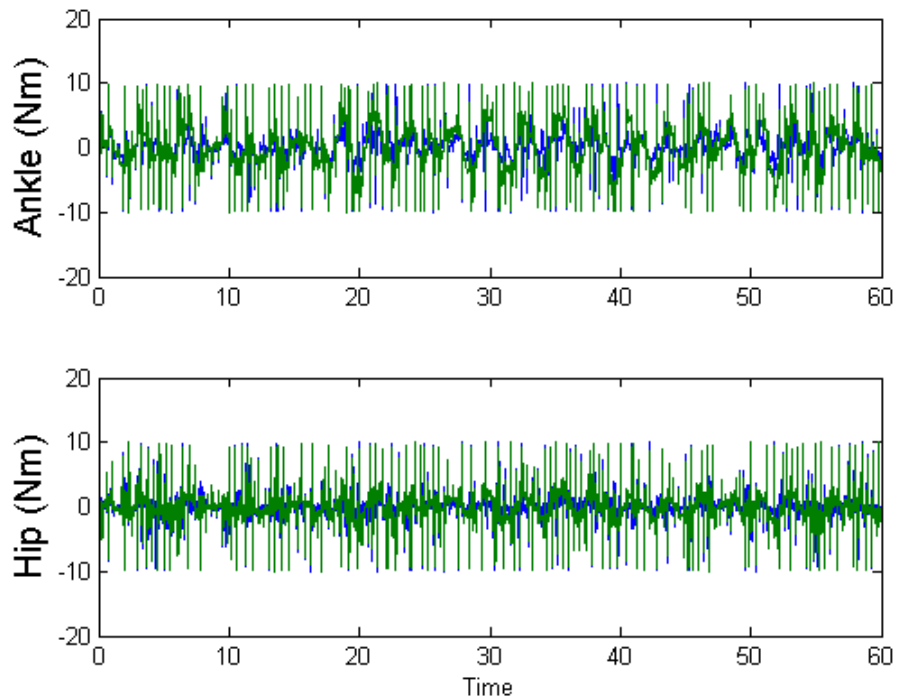


FIGURE 5.6: Control signal, the blue is the open eyes test and green line the closed eyes test.

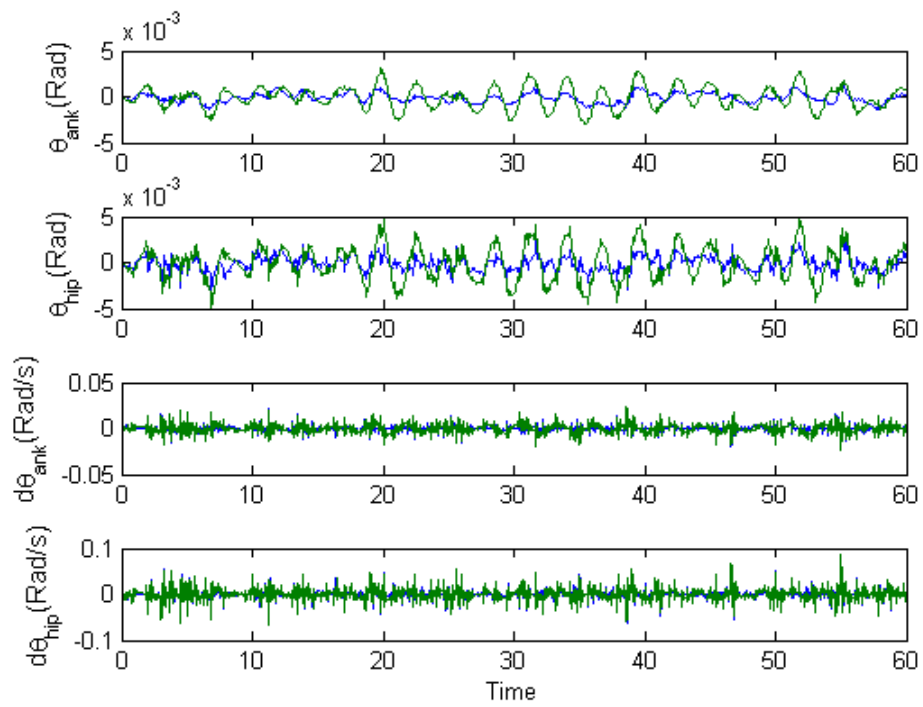


FIGURE 5.7: States signals, the blue is the open eyes test and green line the closed eyes test.

6 | Experiment Protocol

Based on the construction of the model an experiment protocol is suggested in order to validate and adjust the model.

6.1 Participants Conditions

Due to the purpose of this project is describing the normal posture, it must be ensured that people who participate in the experiment satisfy the requirements of a healthy human. Therefore, a selection of a group aged between 20 and 25 with the percentage of fat and the percentage of water are within the normal parameters [4], guaranteeing the maximum physical development without apparent deterioration.

Based on studies by physiologists cited in each point, the experiment was developed with the following features:

- The person must be measured after breakfast, between 8:00am to 11:00pm[22].
- The person must have slept at least 7 hours [25].
- The measures are taken by using the Roomberg test¹[12].
- The participants of the test must be: in an age range of 20-25 and separated in two groups (men and women)[2].
- The person must not have metabolic alterations like: Diabetes, hypertension, fluid retention, pregnancy, etc.

According to the Colombian laws [26], the risks of the procedure must be evaluated to standardize the protocol. The law definitions establish that this procedure is considered as a low risk since the measures are taken with a physical exam.

The law, excludes low risk experiments of informed consent with a justification from the ethics committee.

6.2 Measures

In order to compare the model with the participant measurements, the data of the ankle and hip angles must be recorded. It is recommendable taking the measures in a specialized gait analysis laboratory since this kind of laboratory have cameras and the specialized software calibrated to take the measures.

¹upright standing for a minute, first with the eyes open, then with the eyes closed.

The measures can be made with other kind of sensors. In [27] is suggested the use of inertial measure unit in order to get the angles but the use of accelerometers reduce the precision for small angles and even the position in the body may affect the measure. Also, in [23] the laser sensor are used to analyze the body sway but the sensors have to be moved in order to take different measures in different people. On the other hand, the laser sensor have high resolution.

The following table summarize the sensors used in some researches regarding to postural sway.

TABLE 6.1: Some sensors used to measure the postural sway.[28]

Sensor Type	Postural Stability Measures	Modality
Inertial Sensor Freq: 128Hz Shank	RMS acceleration Anteroposterior	Dynamic Postureography
3D Accelerometer Freq: 20 Hz Sternum Front pelvis, Back pelvis	RMS acceleration For sum of sternum accelerations For sum of front pelvis accelerations For sum of back pelvis accelerations RMS Jerk For sum of sternum accelerations	Gait
3D Accelerometer Freq: 113 Hz Lower back	Length of sway Maximum sway distance Mean sway distance Maximum linear velocity	Quite Stance
1D Gyroscopes Freq: 200 Hz Anterior shank 2D Gyroscopes Freq: 200 Wrist	Maximum Angular velocity ratio	Gait
3D Accelerometer Freq:100 Hz	Harmonic ratio (HR) Anteroposterior (AP) Mediolateral (ML) Vertical (VT) Stride regularity Stride timing variability	Gait

The table 6.1 shows that is common the use of accelerometers to measure the postural sway, but in this application it is not only necessary the measure of the linear displacement, also is necessary the angular displacement. Regarding to this, is suggested to use a inertial measure unit (IMU) to take the measures.

Most of the measures taken in the table 6.1 suggest that the sampling time to measure the postural sway is $200Hz$, and taking into account the simulation in the chapter 5, the gyroscope must be able to measure angles less than 0.1° . The IMU MPU6050 is able to take those kind of measures because it have a high precision 3-Axis gyroscope ($0.01^\circ/LSB$) and a 3-Axis accelerometer ($\pm 2g$). To take the measures are necessary two sensors, one for the truck segment and another for the leg segment.

6.3 Validation and Adjustment

To test the model, first is necessary to introduce the height and weight of the person to be evaluated. The model computes the optimal control for those characteristics, simulates the natural sway and evaluates the covariance ellipse. After, the measures of the participant must be written as a covariance ellipse and both ellipses are compared.

First case: if the person is healthy the ellipse of the measures must be similar or smaller than the ellipse of the model. That means that the model is correct and the person has a normal or greater balance.

Second case: if the person is healthy and the ellipse of the measures is bigger than the ellipse of the model. That means that the model must be adjusted in order to reach the ellipse of the healthy person.

7 | Conclusions and Future Work

With the literature review it was possible to develop a double inverted pendulum model for analyzing posture in sagittal position. The most influential joints in balance control are the ankle and hip, which were selected as the two pins of the pendulum. With the model it was possible to develop an LQR controller to stabilize the double inverted pendulum similar to that of a human.

Then, by adding natural sensors it was possible to create an estimator taking into account the dynamics of natural body sensors like vision, the vestibular system and proprioception. Finally, by combining the controller and the estimator it was possible to simulate the natural roll of the human body with similar characteristics to those described in the literature.

- As a main achievement, the double inverted pendulum model was controlled, due that the model was designed with the anthropometric features of average people and this study was developed using validated research from other publications, the approximated model is suitable to continue with the balance control analysis.
- Using an estimation of the state variables based on the real sensors was possible to simulate the approximated behavior of the human body upright position. Also, simulate the effect in the control balance for different people based on the height and weight was possible too.
- By taking into account the anthropometric characteristics of human beings in the development of the model, this allows to scale and modify the model according to the characteristics of the person being assessed.
- To validate and adjust the model it is crucial to count with precise measurements; this is why it is recommended the use of a specialized laboratory. Other sensors may be used nonetheless results variation is a possible risk due to the complications of instrument calibration for each subject studied.
- Although some authors focus on the analysis of the center of mass or center of pressure to analyze the stability, taking these parameters is not enough for proper study because they omit information about the actual position of body parts.
- Different uses of models such as the one developed in this project can be extended to the development of drivers for the stabilization of bipedal robots or construction of exoskeletons to help stabilization.
- It is not enough to address the problem theoretically, is necessary to adjust the model, taking steps in validation on real people. Although the literature gives information about natural sensors used in the human body, these have not yet been fully characterized and so are critical parameters in the model's performance.
- In order to address other characteristics of stability it is recommended that an analysis of the posture in the frontal position and thus complete the model in three dimensions.

Bibliography

- [1] David G Armstrong and Benjamin A Lipsky. Preventing Foot Ulcers in Patients With Diabetes. 293(2):217–228, 2014.
- [2] Hewstone Miles, Frank D. Fincham, and Jonathan Foster. *Psychology*. 2005. ISBN 978-0-631-20678-1.
- [3] Ji Won Kim, Gwang Moon Eom, Chul Seung Kim, Da Hye Kim, Jae Ho Lee, Byung Kyu Park, and Junghwa Hong. Sex differences in the postural sway characteristics of young and elderly subjects during quiet natural standing. *Geriatrics and Gerontology International*, 10(2):191–198, 2010. ISSN 14441586.
- [4] AS Jackson and ML Pollock. Practical assessment of body composition. *Gait & posture*, 1985.
- [5] David a. Winter. *Biomechanics and motor control of human movement*. Fourth edition, 2009. ISBN 047144989X.
- [6] William H. Gage, David a. Winter, James S. Frank, and Allan L. Adkin. Kinematic and kinetic validity of the inverted pendulum model in quiet standing. *Gait and Posture*, 19:124–132, 2004. ISSN 09666362.
- [7] Tjitske Anke Boonstra, Alfred C Schouten, and Herman van der Kooij. Identification of the contribution of the ankle and hip joints to multi-segmental balance control. *Journal of neuroengineering and rehabilitation*, (1):23. ISSN 1743-0003.
- [8] Matjai Mihelj and Marko Munih. Double Inverted Pendulum Optimal Control - Basis for Unsupported Standing. *Motion Control, 2002. 7th International*, (2):121–126, 2002.
- [9] Alberto Leardini, John J O'Connor, and Sandro Giannini. Biomechanics of the natural, arthritic, and replaced human ankle joint. *Journal of foot and ankle research*, 7(1):8, January 2014. ISSN 1757-1146.
- [10] Ilona J Pinter, Roos Van Swigchem, A J " Knoek, Van Soest, and Leonard A Rozendaal. The Dynamics of Postural Sway Cannot Be Captured Using a One-Segment Inverted Pendulum Model: A PCA on Segment Rotations During Unperturbed Stance. *J Neurophysiol*, 100:3197–3208, 2008.
- [11] Human standing: does the control strategy preprogram a rigid knee? *Journal of applied physiology (Bethesda, Md. : 1985)*, 114(12):1717–29, 2013. ISSN 1522-1601.
- [12] Da Winter. Human balance and posture control during standing and walking. *Gait & Posture*, 3(4):193–214, 1995. ISSN 09666362.
- [13] a. D. Kuo. An optimal control model for analyzing human postural balance. *IEEE Transactions on Biomedical Engineering*, 42(1):87–101, 1995. ISSN 00189294.
- [14] Michael Paulin. A kalman filter theory of the cerebellum. In MichaelA. Arbib and Shunichi Amari, editors, *Dynamic Interactions in Neural Networks: Models and Data*, volume 1 of *Research Notes in Neural Computing*, pages 239–259. Springer New York, 1989. ISBN 978-0-387-96893-3.

- [15] John S. Bay. *Fundamentals of Linear State Space Systems*. First edition, 1999.
- [16] Arthur D Kuo. An optimal state estimation model of sensory integration in human postural balance. *Journal of neural engineering*, 2(3):S235–S249, 2005. ISSN 1741-2560.
- [17] GP McRuer, DT, Magdaleno, RE, Moore. A neuromuscular actuation system model. *Man-Machine Systems, . . .*, MMS-9(3):61–71, 1968. ISSN 0536-1540.
- [18] C Fernandez and J M Goldberg. Physiology of peripheral neurons innervating semicircular canals of the squirrel monkey. II. Response to sinusoidal stimulation and dynamics of peripheral vestibular system. *Journal of neurophysiology*, 34(4):661–675, 1971. ISSN 0022-3077.
- [19] J W Grant and J R Cotton. A model for otolith dynamic response with a viscoelastic gel layer. *J. Vestib. Res.-Equilib. Orientat.*, 1(2):139–151, 1990. ISSN 0957-4271.
- [20] Shin-ichi Demura, Tamotsu Kitabayashi, and Hiroki Aoki. Body-sway characteristics during a static upright posture in the elderly. *Geriatrics & Gerontology International*, 8(3):188–197, 2008. ISSN 14441586.
- [21] H Røgind, J J Lykkegaard, and H Bliddal. Postural sway in normal subjects aged 20 – 70 years. pages 171–176, 2003.
- [22] Pia Forsman, Edward Haeggström, Anders Wallin, Esko Toppila, and Ilmari Pyykkö. Day-time changes in postural stability and repeatability of posturographic measurements. *Journal of occupational and environmental medicine / American College of Occupational and Environmental Medicine*, 49(6):591–596, 2007. ISSN 1076-2752.
- [23] BL Day and MJ Steiger. Effect of vision and stance width on human body motion when standing: implications for afferent control of lateral sway. *The Journal of . . .*, pages 479–499, 1993.
- [24] Y Aramaki, D Nozaki, K Masani, T Sato, K Nakazawa, and H Yano. Reciprocal angular acceleration of the ankle and hip joints during quiet standing in humans. *Experimental brain research. Experimentelle Hirnforschung. Experimentation cerebrale*, 136:463–473, 2001. ISSN 0014-4819.
- [25] M Patlak. Your guide to healthy sleep. *US Department of Health and Human Services*, 2005.
- [26] Republica de Colombia. Resolucion 8430 de 1993 - 1. 1993:1–12, 1993.
- [27] Weijun Tao, Tao Liu, Rencheng Zheng, and Hutian Feng. Gait Analysis Using Wearable Sensors. *Sensors*, 12(12):2255–2283, 2012. ISSN 1424-8220.
- [28] Ryan P Hubble, Geraldine A Naughton, Peter A Silburn, and Michael H Cole. Wearable sensor use for assessing standing balance and walking stability in people with Parkinson’s disease: a systematic review. *PloS one*, 10(4):e0123705, 2015. ISSN 1932-6203. doi: 10.1371/journal.pone.0123705.